Optica Applicata, Vol. LIV, No. 3, 2024
DOI: 10.37190/oa240306

Optimizing LED spectrum fitting using double Gaussian functions

Jianxiao Liu[1,3,*], Mingmin Su[1], Yan Jiang[2], Jingjing Du[1,*], Xiaolan Liu[1], Ziyue Yao[1], Ruijie Deng[1], Jiaqi Shen[1], Xin Liu[1]

[1]School of Electronics and Information Engineering, Hengshui University, Hengshui 053000, People's Republic of China

[2]College of Integrated Circuit Science and Engineering, Nanjing University of Posts and Telecommunications, Nanjing 210023, People's Republic of China

[3]Collaborative Innovation Center for Wetland Conservation and Green Development of Hebei Province, Hengshui 053000, People's Republic of China

*Corresponding author: lxf9431@sina.com (L.J.), 249242895@qq.com (D.J.)

In order to minimize errors during the LED spectrum fitting process and achieve a closer match between the fitted spectrum and the target spectrum, a method employing double Gaussian functions for fitting is proposed. This approach, in comparison to the widely applied modified Gaussian model, avoids issues such as sidelobe uplift when dealing with narrow-band LED spectra. It demonstrates effective fitting for narrow-band LED spectra, exhibiting higher fitting accuracy at the bottom of the spectrum compared to the simple Gaussian model. Moreover, this fitting method introduces no additional fitting variables. The model is constructed by combining two Gaussian functions with weighted summation, and optimizing the weighted coefficients of the two Gaussian functions achieves the best fitting results. Finally, the proposed model is applied to fit various LED spectra, yielding satisfactory results. The outcomes indicate that the overall fitting performance of the double Gaussian model surpasses that of the Gaussian model and the modified Gaussian model.

Keywords: LED, spectrum fitting, Gaussian functions.

1. Introduction

LED technology, characterized by its low cost, compact spectrum, and low power consumption, has gained extensive applications. The utilization of LED spectra fitting, meeting production and research requirements, has gradually become a research focus [1-3]. Tsuno *et al*. simulated solar spectra using LEDs, demonstrating higher efficiency and longer usage periods compared to traditional light sources. Kolberg *et al*. achieved measurements close to real solar spectra using LED sources [4-6]. At present, optimi-

zation algorithms enable fitting any target spectrum, as demonstrated by ZHU JIYI, GAN RUTING, and others [7-8]. These studies, centered around LED spectra, emphasize the accurate representation of monochromatic LED spectral characteristics to enhance fitting precision. Currently, Gaussian models and modified Gaussian models are the primary approaches for LED spectral fitting [9-12].

Gaussian model:

$$S(\lambda) = \exp\left(-2.7726\left(\frac{\lambda-\lambda_0}{\Delta\lambda}\right)^2\right) \tag{1}$$

Modified Gaussian model:

$$S(\lambda) = \exp\left(-3.2213\left(\frac{\lambda-\lambda_0}{\Delta\lambda}\right)^2 \exp\left(-0.3\left|\frac{\lambda-\lambda_0}{\Delta\lambda}\right|\right)\right) \tag{2}$$

Where $S(\lambda)$ is the normalized spectral distribution, λ_0 is the peak wavelength, and $\Delta\lambda$ is the full width at half maximum (FWHM). Peak wavelength and FWHM are two crucial parameters of the LED spectrum curve. Based on the radiation characteristics of LED sources, there exists a wavelength corresponding to the peak radiation intensity, known as the peak wavelength λ_0. It is generally determined by the level position of the emitting center in the semiconductor material and represents the color of the LED. The spectral FWHM is the difference between the wavelengths corresponding to the two half-peak positions on the relative spectral distribution curve, indicating the spectral purity of monochromatic LEDs. In the early stages of LED spectrum research, Gaussian models were often used to fit the spectral curves [13]. However, due to significant differences between the Gaussian model and the actual LED spectrum curve at the bottom of the spectrum, researchers proposed a method using the modified Gaussian model for fitting [14]. While the introduction of the modified Gaussian model improved the accuracy of spectrum fitting to some extent, it also brought about a critical issue.

With the development of the LED industry, the production processes for LEDs with excellent monochromaticity have matured. Higher monochromaticity implies a smaller $\Delta\lambda$. When $\Delta\lambda$ becomes sufficiently small, the modified Gaussian model can no longer effectively fit the LED spectrum. This is particularly evident in the problem of sidelobe uplift in fitting narrow-band LEDs. To overcome this issue, this study proposes a method using the weighted fitting of two Gaussian functions [15-16]. The results indicate that the dual Gaussian model can effectively fit any narrow-band LED spectrum with high accuracy.

2. Sidelobe uplift issue in the modified Gaussian model spectrum

Taking the wavelength range as the abscissa from 380 to 780 nm and the FWHM as the ordinate, with values ranging from 10 to 20 nm, normalized spectra were plotted

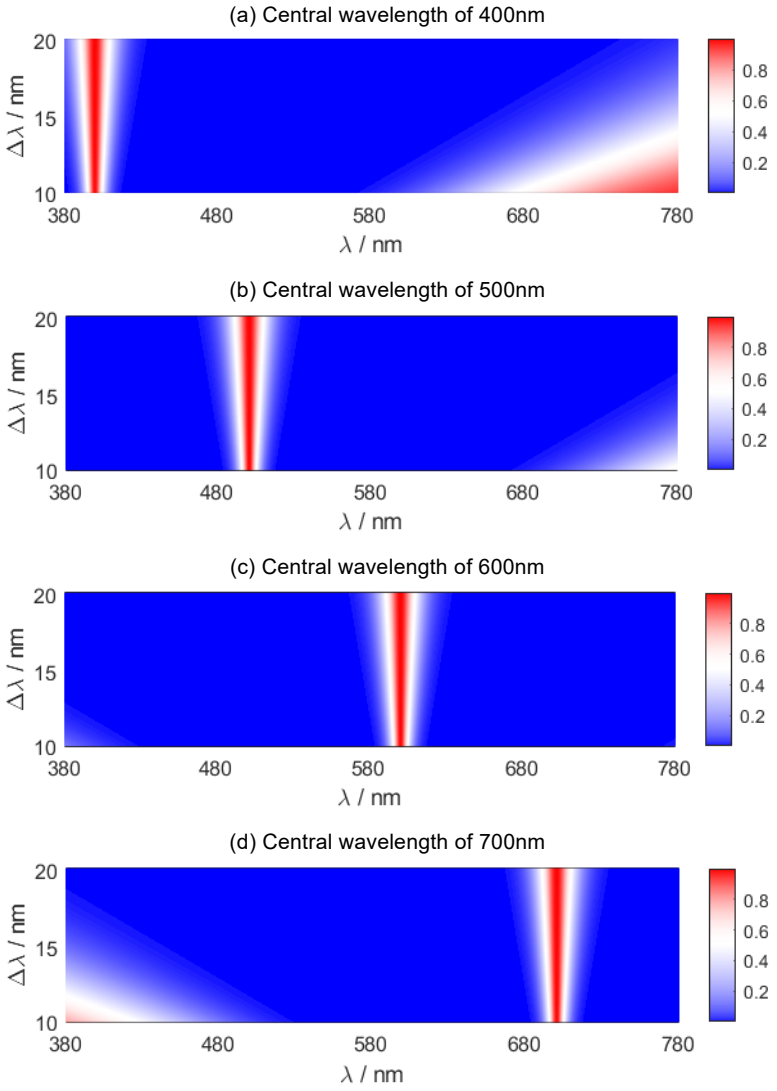

Fig. 1. Simulation of LED Spectrum using the modified Gaussian model. Central wavelengths are respectively set to (a) 400 nm, (b) 500 nm, (c) 600 nm, and (d) 700 nm.

for peak wavelengths of 400, 500, 600, and 700 nm. It can be observed that when the peak wavelength is set to 400 nm (Fig. 1(a)), a problem of sidelobe uplift occurs in the long wavelength range of 580 to 780 nm. In this range, there is an undesired spectral distribution where the intensity should ideally be zero. This issue becomes more severe when the FWHM is smaller and is alleviated as the FWHM increases. As the central wavelength increases, sidelobe uplift gradually diminishes when the central wavelength is set to 500, 600, and 700 nm (Figs. 1(b)–(d)). However, when the central wavelength

is set to 700 nm (Fig. 1(d)), sidelobe uplift appears in the short wavelength range of 380 to 480 nm. Additionally, in Fig. 1(d), when the FWHM is set to 10–15 nm, an undesired spectral distribution is observed where it should not exist.

The modified Gaussian model $S(\lambda)$ is conceived as an even function $S_0(\lambda)$ initially translated along the horizontal axis by λ_0 and then stretched by a factor of $\Delta\lambda$. $S_0(\lambda)$ is as follows:

$$S_0(\lambda) = \exp\left(-3.2213(\lambda)^2 \exp(-0.3|\lambda|)\right) \tag{3}$$

Obviously, the modified Gaussian model exhibits a symmetrical distribution about the central wavelength λ_0. Within the real number range, this function possesses one maximum (λ_0, 1) and two minima.

To facilitate the determination of the coordinates corresponding to the minima, we take the natural logarithm of the function $S(\lambda)$.

Letting $f(\lambda) = \ln[S(\lambda)]$, then

$$f(\lambda) = \ln[S(\lambda)] = -3.2213\left(\frac{\lambda-\lambda_0}{\Delta\lambda}\right)^2 \exp\left(-0.3\left|\frac{\lambda-\lambda_0}{\Delta\lambda}\right|\right) \tag{4}$$

Resulting in its derivative:

$$f'(\lambda) = \begin{cases} \dfrac{6.4426(\lambda-\lambda_0)\exp\left[-0.3\left(\dfrac{\lambda-\lambda_0}{\Delta\lambda}\right)\right]}{\Delta\lambda^2} - \dfrac{0.96639\exp\left[-0.3\left(\dfrac{\lambda-\lambda_0}{\Delta\lambda}\right)\right]\left(\dfrac{\lambda-\lambda_0}{\Delta\lambda}\right)^2}{\Delta\lambda} & (\Delta\lambda < \lambda_0) \\ \dfrac{6.4426(\lambda-\lambda_0)\exp\left[-0.3\left(\dfrac{\lambda-\lambda_0}{\Delta\lambda}\right)\right]}{\Delta\lambda^2} + \dfrac{0.96639\exp\left[-0.3\left(\dfrac{\lambda-\lambda_0}{\Delta\lambda}\right)\right]\left(\dfrac{\lambda-\lambda_0}{\Delta\lambda}\right)^2}{\Delta\lambda} & (\Delta\lambda > \lambda_0) \end{cases} \tag{5}$$

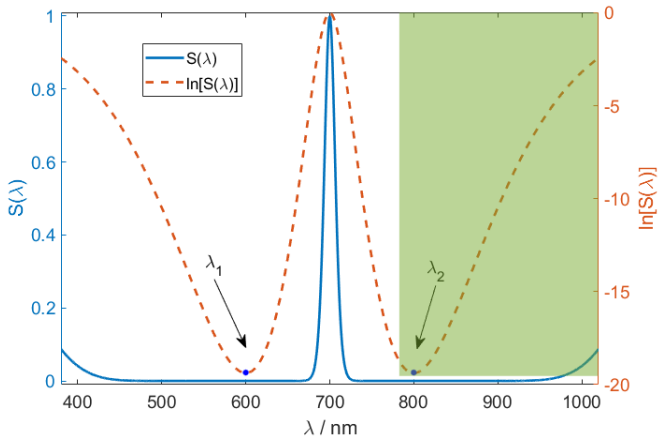

Fig. 2. The explanation for the sidelobe uplift in the modified Gaussian model.

Using $f'(\lambda) = 0$, we obtain

$$\begin{cases} \lambda_1 = \lambda_0 - \dfrac{20}{3}\Delta\lambda & (\lambda_1 < \lambda_0) \\ \lambda_2 = \lambda_0 + \dfrac{20}{3}\Delta\lambda & (\lambda_2 > \lambda_0) \end{cases} \tag{6}$$

For instance, when the central wavelength $\lambda_0 = 700$ nm and $\Delta\lambda = 15$ nm, we obtain $\lambda_1 = 600$ nm and $\lambda_2 = 800$ nm, as depicted in Fig. 2. Notably, only λ_1 falls within the wavelength range of 380–780 nm. For $\lambda < \lambda_1$, $S(\lambda)$ gradually increases, deviating from the typical LED spectral characteristics. Conversely, λ_2 lies beyond the computed range, indicated by the green region in Fig. 2. Thus, we only observe the sidelobe uplift in the short wavelength range of 380 to 480 nm.

Similarly, when the central wavelength $\lambda_0 = 400$ nm, 500 nm, *etc*., the function's axis of symmetry shifts towards shorter wavelengths. At this juncture, the sidelobe uplift manifests in the long wavelength range.

From the above analysis, it is evident that when using the modified Gaussian model, there is a sidelobe uplift issue in the spectral distribution, particularly when the FWHM $\Delta\lambda$ is small, corresponding to narrow-band LEDs. In such cases, the model fails to accurately describe the spectral distribution of LEDs. Figure 3 illustrates the spectral distribution when the peak wavelength is set to 400 nm, and FWHM values are 25, 20, 18, and 15 nm. It can be observed that when $\Delta\lambda$ is less than 25 nm, there are significant errors in the long-wavelength spectrum.

Figure 4 presents the spectral distribution when the peak wavelengths are set to 500, 450, 400, and 380 nm, with an FWHM of 18 nm. When the central wavelength λ_0 shifts towards shorter wavelengths, sidelobe uplift appears in the long wavelength range (highlighted by red ellipses in the figure). For example, when λ_0 is respectively set to 450,

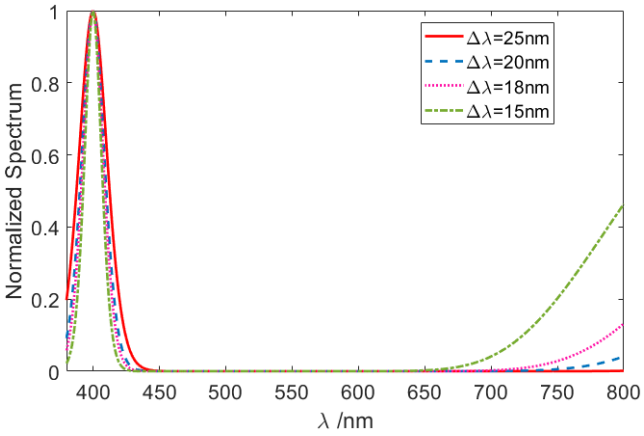

Fig. 3. Simulation of different LED spectra with varying FWHM using the modified Gaussian model.

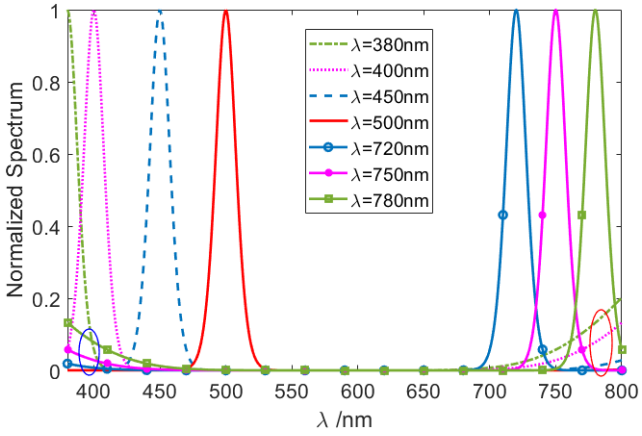

Fig. 4. Simulation of different LED spectra with varying peak wavelength using the modified Gaussian model.

400, and 380 nm, the LED spectrum exhibits uplift between 700 and 800 nm. Conversely, as the central wavelength shifts towards longer wavelengths, sidelobe uplift occurs in the short wavelength range (highlighted by blue ellipses in the figure). For instance, when λ_0 is respectively set to 720, 750, and 780 nm, the LED spectrum experiences uplift between 380 and 480 nm. Only within the range of 450 nm < λ_0 < 720 nm does the effect of sidelobe uplift on the spectrum remain minimal, as illustrated by the red line in the figure corresponding to λ_0 is 500 nm.

3. Dual Gaussian model

Five types of LEDs were randomly selected and their spectral distributions were measured in a 25°C environment. The central wavelength and FWHM of the LEDs are shown

T a b l e 1. LED spectrum parameters.

Parameter	LED1	LED2	LED3	LED4	LED5
Central wavelength [nm]	463.3	527.7	571.8	625.5	641.7
FWHM [nm]	24.7	32.6	18.6	18.2	18.7

T a b l e 2. Fitting coefficients of the dual Gaussian model for LED spectra (from Table 1).

Fitting coefficients	LED1	LED2	LED3	LED4	LED5	Mean
Weight α	0.6339	0.6705	0.7639	0.7494	0.7204	0.7076
Coefficient β_1	4.4358	4.4561	3.8920	3.8533	4.2287	4.1732
Coefficient β_2	0.9391	0.9764	0.8150	0.8555	0.7872	0.8746
Residual ε	0.0434	0.3536	0.0740	0.0947	0.2532	0.1560

Note: α represents the weights, β_1 is the coefficient of the first Gaussian function, β_2 is the coefficient of the second Gaussian function, and the residual ε for each LED spectrum, respectively. The "Mean" column provides the average values across all LEDs.

in Table 1. Spectral fitting was conducted using a dual Gaussian model. The model is expressed as follows.

Dual Gaussian model:

$$S(\lambda) = \alpha \exp\left[-\beta_1\left(\frac{\lambda-\lambda_0}{\Delta\lambda}\right)^2\right] + (1-\alpha)\exp\left[-\beta_2\left(\frac{\lambda-\lambda_0}{\Delta\lambda}\right)^2\right] \tag{7}$$

From the averaged fitting coefficients in Table 2, it is observed that the mean values for the weight α, coefficient β_1, and coefficient β_2 are 0.7076, 4.1732, and 0.8746, respectively. Using these mean coefficients as the fitting parameters for the dual Gaussian model, a re-fitting was performed on the five types of LEDs. The results were then compared with two other models, and the fitting results and error distributions are presented in Fig. 5. The left panel shows the fitting results of the measured LED values with the three models, while the right panel displays the absolute errors between the measured values and the fitted results. The method for calculating the absolute errors is as follows:

$$\text{Absolute error} = |\text{Measured value} - \text{Fitted value}| \tag{8}$$

Due to the asymmetrical distribution of LED spectra around the peak wavelength, all three models exhibit some degree of error at the bottom of the spectra. The modified Gaussian model reduces errors at the bottom of the spectrum to some extent but introduces sidelobe uplift issues for narrow-band LEDs. The dual Gaussian model, utilizing the weighted combination of two Gaussian functions, reduces errors at the bottom of the LED spectrum and simultaneously addresses the sidelobe uplift issue seen in the modified Gaussian model. As shown in the error distribution in Fig. 5, among the three

Fitting results and absolute error for LED1 spectrum

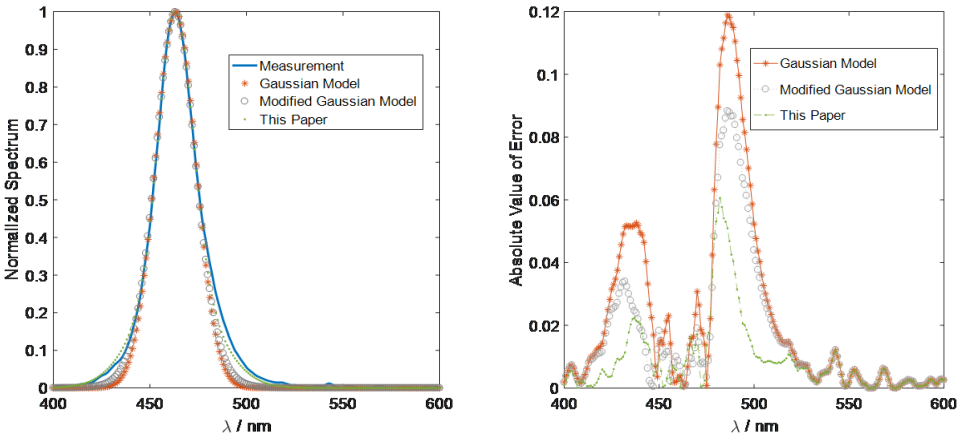

Fitting results and absolute error for LED2 spectrum

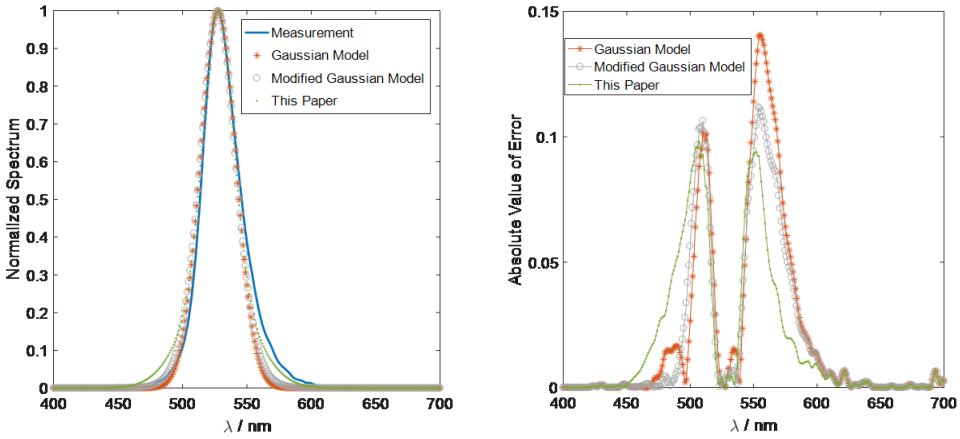

Fitting results and absolute error for LED3 spectrum

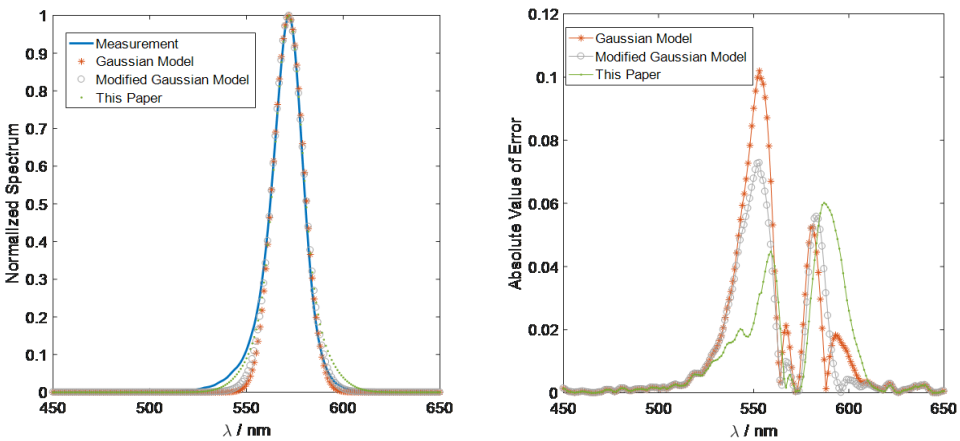

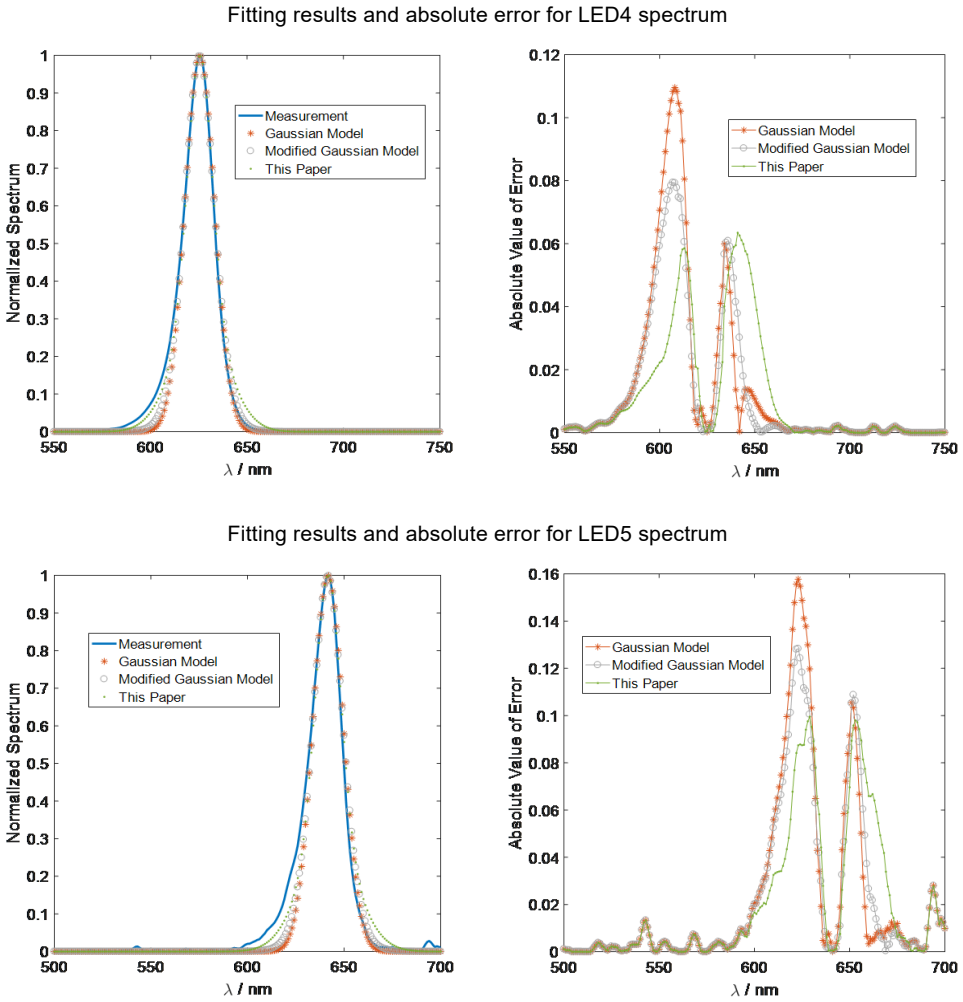

Fig. 5. LED spectrum fitting and error distribution.

fitting models, the simple Gaussian model has the highest error, followed by the modified Gaussian model, while the dual Gaussian model exhibits the smallest errors.

The fitting results and errors distribution of the three spectral models in Fig. 5 indicate that the fitting results using the dual Gaussian model are overall superior to the other two spectral models. Figure 6 illustrates the LED spectra simulated using the dual Gaussian model. The central wavelengths are set to 400 and 700 nm, with FWHM $\Delta\lambda$ values ranging from 10 to 20 nm. It can be observed from the figure that when the central wavelength is close to the sidelobes, the dual Gaussian model does not exhibit the sidelobe uplift issue seen in the modified Gaussian model.

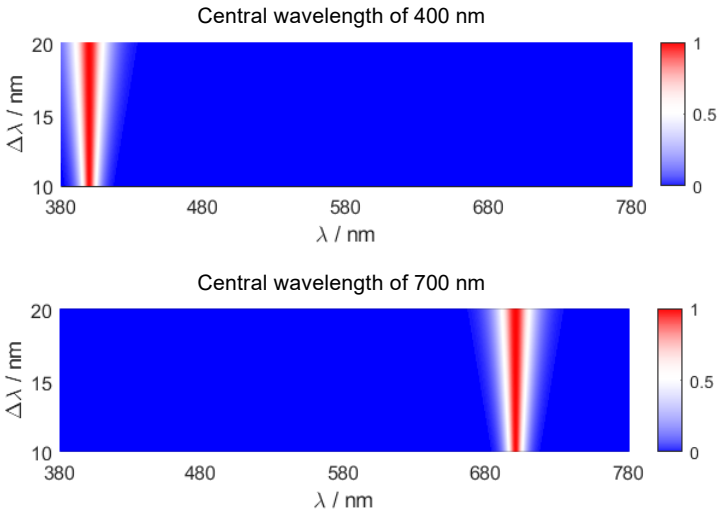

Fig. 6. LED spectra simulated using the dual Gaussian model with central wavelengths at 400 and 700 nm.

4. Conclusion

This paper introduces a novel LED spectrum fitting model that, overall, outperforms the widely used modified Gaussian model in terms of fitting accuracy. The proposed model tackles sidelobe elevation observed in the long-wavelength band when the central wavelength shifts to shorter wavelengths. Similarly, it addresses the sidelobe elevation in the short-wavelength band when the central wavelength shifts to longer wavelengths. By fitting the spectra of five randomly selected LEDs, parameters for the dual Gaussian model were obtained. The simplicity and computational efficiency of this model make it particularly suitable for fitting narrow-band LED spectra. It is recommended for broader application in engineering practices involving spectrum fitting and related areas.

Funding
This work was supported by the Natural Science Foundation of Hebei Province Youth Fund (Grant No. F2019111025, No. F2021111001), Science Research Project of Hebei Education Department (Grant No. QN2023056), and the Hengshui University High Level Talent Launch Fund (Grant No. 2023GC04).

Disclosures
The authors declare no conflicts of interest.

Data availability
Data available on request from the authors.

References

[1] SUN C., JIN Z., SONG Y., CHEN Y., XIONG D., LAN K., HUANG Y., ZHANG M., *LED-based solar simulator for terrestrial solar spectra and orientations*, Solar Energy **233**, 2022: 96-110. https://doi.org/10.1016/j.solener.2022.01.001

[2] Rghif Y., Bahraoui F., Zeghmati B., *Experimental and numerical investigations of heat and mass transfer in a salt gradient solar pond under a solar simulator*, Solar Energy **236**, 2022: 841-859. https://doi.org/10.1016/j.solener.2022.03.033
[3] Bliss M., Betts T.R., Gottschalg R., *Advantages in using LEDs as the main light source in solar simulators for measuring PV device characteristics*, Proceedings of the SPIE, Vol. 7048, Reliability of Photovoltaic Cells, Modules, Components, and Systems, 2008: 704807. https://doi.org/10.1117/12.795428
[4] Tsuno Y., Kamisako K., Kurokawa K., *New generation of PV module rating by LED solar simulator—A novel approach and its capabilities*, [In] *2008 33rd IEEE Photovoltaic Specialists Conference*, San Diego, CA, USA, 2008: 1-5. https://doi.org/10.1109/PVSC.2008.4922582
[5] Kolberg D., Schubert F., Klameth K., Spinner D.M., *Homogeneity and lifetime performance of a tunable close match LED solar simulator*, Energy Procedia **27**, 2012: 306-311. https://doi.org/10.1016/j.egypro.2012.07.068
[6] Fryc I., Brown S.W., Eppeldauer G.P., Ohno Y., *LED-based spectrally tunable source for radiometric, photometric, and colorimetric applications*, Optical Engineering **44**(11), 2005: 111309. https://doi.org/10.1117/1.2127952
[7] Zhu J.Y., Ren J.W., Li B.Y., Wan Z., Liu Z.X., Li X.S., Zhang Y.Q., Zhao Y.E., Quan X.R., *Synthesis of spectral distribution for LED-based source with tunable spectra*, Chinese Journal of Luminescence **31**, 2010: 883-887. (in Chinese)
[8] Gan R.T., Guo Z.N., Lin J.B., Zheng M.J., Yang F.F., Yan W.P., Lin M.C., *The genetic algorithm in the applicationg of LED light source spectral maching technology*, Acta Photon Sinica **43**, 2014: 0730003. (in Chinese)
[9] Huang M.L., Chen H.T., Zhou X.F., Cai J.Y., Zhou J.R., He Z.Q., *Optimization spectrum of white light emitting diodes based on correlated color temperature and luminous flux*, Acta Photonica Sinica **44**, 2015: 1030001. (in Chinese)
[10] Ren Z.M., Lu H.M., Feng L.Y., Yang L., Zhu Y.F., Wang J.P., *A method for natural spectral reproduction based on fully connected neural network*, Acta Optica Sinica **43**, 2023: 1030001. (in Chinese)
[11] Chen X.C., *Improved bounding box regression loss function based on smooth L1*, College Mathematics **37**, 2021: 18-23. (in Chinese)
[12] Zhang Y.B., Dong L., Zhang G.Y., *Simulation of high power monochromatic LED solar spectrum based on effective set algorithm*, Chinese Journal of Luminescence **39**, 2018: 862-869. (in Chinese)
[13] Zhu J.Y., *The Research of LED-based Spectrally Tunable Source*, Master's Degree Thesis of Graduate School of Chinese Academy of Sciences, 2010. (in Chinese)
[14] Shen H.P., Feng H.J., Pan J.G., Hu H.Y., *LED spectral mathematical models and their applications*, [In] *Proceedings of 26th Annual Meeting of Chinese Illuminating Society*, Beijing, China, 2005: 83-85.
[15] Cheng Z., Si G.S., Li Z.G., Ning Z.Q., Liu J.X., Huang W.B., Si B.B., Yang C.P., Fang Y.H., *LED spectral matching based on adaptive differential evolution algorithm*, Acta Optica Sinica **42**, 2022: 0930004. (in Chinese)
[16] Lu H.L., Guo Z.Q., Dang J.S., Gao Y.L., Lu Y.J., *Research on high S/P of phosphor-type white LED with high color temperature*, Electro-Optic Technology Application **31**, 2016: 24-28.

Received February 16, 2024
in revised form April 13, 2024